



Preshock-induced phase transition in spalled U–0.75 wt% Ti

A.K. Zurek *

Materials Research and Processing Science, MST-8 MS: G 755, Los Alamos National Laboratory, Los Alamos, NM 8754, USA

Received 8 September 1997; accepted 22 June 1998

Abstract

Uranium–0.75 wt% Ti samples were spalled in the range of 5–24 GPa shock pressure. One sample was preshocked to a pressure of 24 GPa, ‘soft’ recovered, and then reloaded and spalled at 10 GPa. The spall strength of U–3/4 wt% Ti was found to range from –4.1 to –2.9 GPa when the Romanchenko correction is used in the spall strength calculation. The spall morphology of the sample that was preshocked and then spalled showed a significant change in microstructure from a parent alpha’ martensite to a 2-phase eutectoid. The thermodynamically calculated temperature rise resulting from the preshock at 15–24 GPa in these samples is $\sim 555^\circ\text{C}$. This temperature is not sufficient to induce such a phase change. However, the preshock conditions additionally increase the flow stress of the U–34 wt% Ti, and it is postulated that this additional hardening is sufficient to increase the temperature above 885°C due to the increased amount of plastic work required during spall, thereby triggering the phase change. © 1999 Elsevier Science B.V. All rights reserved.

1. Introduction

Spallation is one of many experimental configurations that can produce controlled dynamic fracture. Spallation is dynamic fracture probe whose stress state is pure uniaxial strain. It occurs in a material due to tensile stresses generated in a mid plane of the sample by the interaction of two release (rarefaction) waves under intensive shock loading conditions [1]. The compressive preshock experiment is designed to precondition a material’s microstructure and resultant yield surface due to shock-induced defect generation and high strain rate while maintaining minimal residual strain in sample [2]. In our preshock experiment at 24 GPa, the residual strain in the sample did not exceed 1.2%. During compressive preshock as well as during the compression portion of the spall cycle, the sample is subjected to severe plastic deformation resulting in an increased post-shock flow stress [3]. This deformation generates a high density of dislocations, and coincidentally generates heat in the sample as a consequence of plastic work involved.

The Rankine–Hugoniot [4,5] relationship can be used to calculate this temperature rise and the residual temperature retained by the sample after the preshock and/or spall cycle is completely released to ambient conditions. These temperature rise effects are important in addition to the defects stored, especially in a material exhibiting a very low heat capacity, such as in refractory metals and particularly in depleted uranium and its alloys. These thermal effects, both during the shock and its release as well as post-shock release, can aid recovery, recrystallization, shear band formation, localized melting on release, post-shock strain aging, reorganization of the substructure [6], as well as influencing phase stability.

The purpose of this paper is to present evidence of a phase change in the post-spalled microstructure of a U–0.75 wt% Ti that was subjected to a preshock at 24 GPa followed by spallation at 10 GPa.

2. Materials and experiments descriptions

U–0.75 wt% Ti material was supplied from Nuclear Metals Incorporated, Concord, Massachusetts. Table 1 lists the chemical composition of the material tested.

The ‘as-received’ U–0.75 wt% Ti was solution heat-treated at 885°C for 2 h and water quenched, followed

* Tel.: +1-505 665 1438; fax: +1-505 667 8021; e-mail: zurek@lanl.gov.

Table 1
Chemical composition of depleted U–0.75 wt% Ti

Uranium	Bulk
Carbon	30 ppm
Nickel	14 ppm
Hydrogen	0.2 ppm
Titanium	0.7 wt%
Iron	14 ppm
Copper	11 ppm

by tempering at 385°C for 4 h. This produced a microstructure composed of α' martensite laths 20–50 μm long containing fine strengthening precipitates of U_2Ti . Fig. 1 shows the microstructure of the as heat-treated U–0.75 wt% Ti prior to the shock experiment [7]. The spall tests were conducted at 298 K in a range of 5–24 GPa shock pressure with a 1- μs pulse duration. A detailed description of the spall tests and the spall strength calculations have been previously presented [7].

3. Results and discussion

Spallation is a process of damage accumulation and linkage that differs drastically from fracture damage in the uniaxial tensile tests by virtue of the stress state and the rate of damage accumulation. In a tensile test, voids and cracks are subject to a nearly uniaxial tensile stress field; homogeneous plastic strain dominates the flow process from an early stage. In a tensile test the hydrostatic stress is of the order of 1/3 the flow stress. In contrast, during spallation, voids or cracks are subject to extremely high, near isotropic, triaxial stresses, and thus to localized high hydrostatic tensile stress fields. How-

ever, the local triaxiality as well as the hydrostatic pressure can be increased in a quasi-static tensile test by introducing deep notches in tensile samples, making this test more ‘comparable’ in stress state (but not in strain rate nor absolute hydrostat magnitude) to a spall test. In addition, a tensile test time scale of events in many orders of magnitude greater than that for a spall test. There is sufficient time for the heat generated during a quasi-static tensile test to be continuously dissipated from the damage region away to the other parts of the sample. The thermodynamically calculated temperature rise produced by shock loading, according to the Rankine–Hugoniot relationship, can be substantial, as shown for many materials in Appendix B of Ref. [6].

Using the same methods as in [6] to calculate the temperature rise in U–0.75 wt% Ti alloy in the current tests, we have estimated that during the compressive preshock at ~ 24 GPa (750 m/s projectile velocity), the sample temperature should increase from 25°C up to $\sim 555^\circ\text{C}$ (see Appendix A). This calculation is very important in the interpretation of the samples’ morphology prior to and after the preshock and spalled conditions.

Fig. 2(a–b) shows a comparison of a parent, quenched aged microstructure U–0.75 wt% Ti (Fig. 2(a)) with the microstructure of the spalled sample (Fig. 2(b)) and the microstructure of the sample preshocked and then spalled (Fig. 2(c)). There is almost no difference in the first two micrographs, and these show the martensitic laths as expected from U–0.75 wt% Ti the heat treatment given to all the samples. The micrograph in Fig. 2(c) however, shows a eutectoid U–0.75 wt% Ti morphology that resembles a microstructure shown previously in Eckelmeyer’s work [8]. This type of microstructure is postulated to have been produced in the equilibrium transformation from $\gamma \Rightarrow \beta + \text{U}_2\text{Ti} \Rightarrow \alpha$

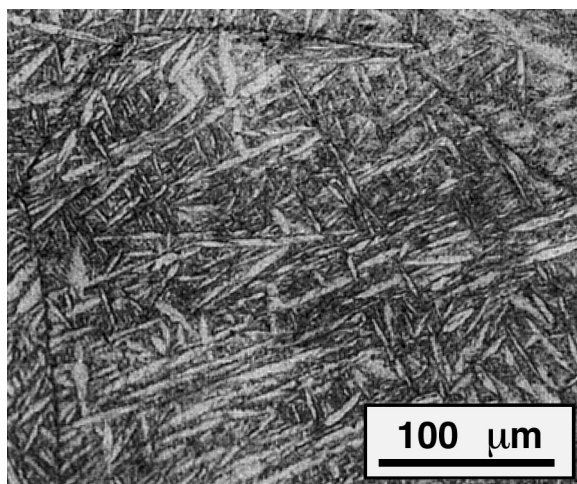


Fig. 1. U–0.75 wt% Ti sample in an annealed condition. The microstructure is composed of α' martensite laths 20–50 μm long and U_2Ti .

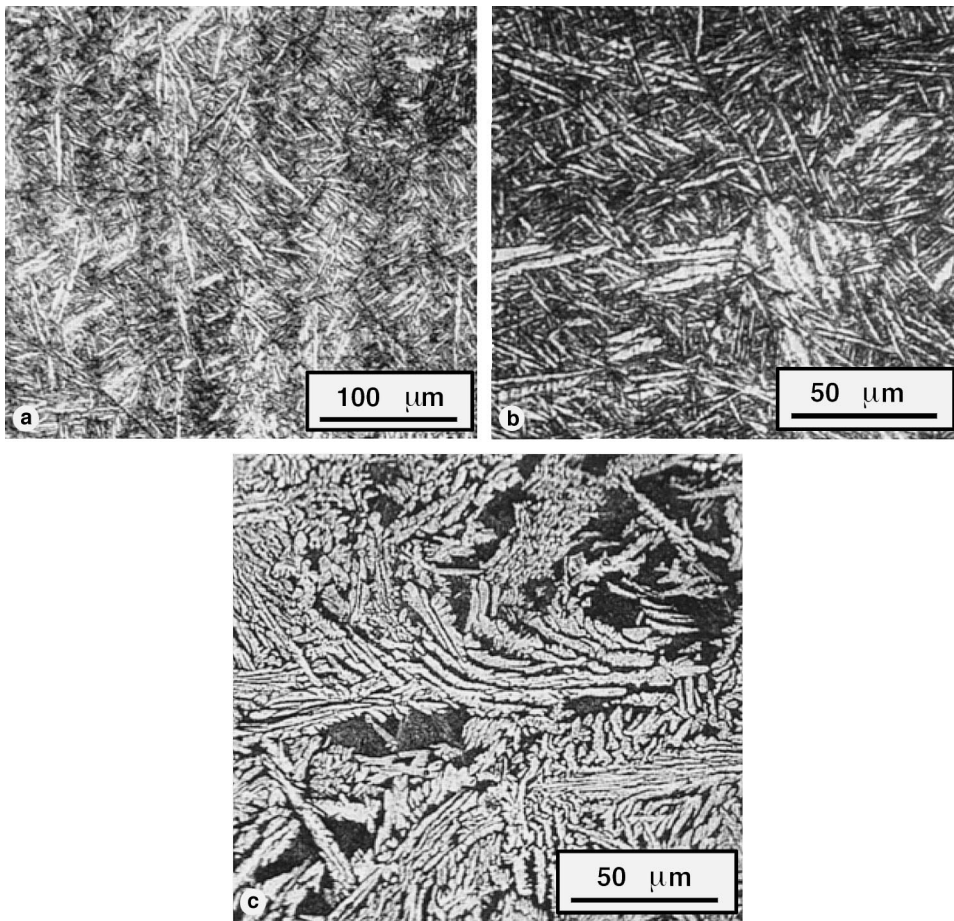


Fig. 2. Optical micrographs showing morphology of material prior to shock loading (a), after a spall test at 10 GPa shock pressure; spall strength -3.6 GPa (b), and after preshock at 24 GPa followed by a spall at 10 GPa shock pressure; spall strength -2.6 GPa (c).

U_2Ti . Under normal equilibrium conditions the initial α' microstructure would have to be heated to $\sim 760^\circ C$ to the γ -phase and then cooled to be transformed to the eutectoid $\alpha + U_2Ti$ phase. As seen in Fig. 2(c), the long white etching lamella are α , and the fine elongated dark needles are a mixture of $\alpha + U_2Ti$.

The shock conditions of both the preshock at 24 GPa pressure and the additional spall at 10 GPa pressure introduced a high density of defects, principally dislocations and thereby increase the overall flow stress level due to the passage of the initial shock. The preshock conditions increased the flow stress of the material almost to its maximum flow stress. We can estimate the strength of shock-hardened material and compare it with that of the same material that has been deformed conventionally at lower strain rates. This calculation and explanation is described by McQueen et al. [9] and Meyers [10]. During the preshock, material goes through a full stress-strain cycle of compression at the front and expansion during the release part of the shock [2,9]. The

preshock test is designed such that the post-shock residual strain in the sample is almost zero (the actual residual strain in our sample was less than 1.2%) [2]. However, the effective total transient strain of the sample at shock is equal: $(\epsilon_{eff})_{total} = \frac{4}{3} \ln V/V_0 = \sim 0.13$ strain, where V_0 and V are initial and shock volumes at 24 GPa shock in U-0.75 wt% Ti [11]. U-0.75 wt% Ti is highly strain rate sensitive only to the strain rate of approximately 2000 1/s as shown by Zurek and Follansbee [12]. At a high strain rate as shown experimentally in Fig. 3 of Ref. [12] and theoretically in Fig. 11 of the same reference [12], at a strain rate of 10^6 1/s (the typical strain rate of the spall test), a flow stress of ~ 2700 MPa could be achieved. The U-0.75 wt% Ti reaches its saturation flow stress at 13% equivalent strain during quasistatic loading. This calculation assumes an equivalent strain of 13% at the 24 GPa pressure in the preshock experiment.

The shock in the spall test following the preshock most likely did not significantly further increase the flow

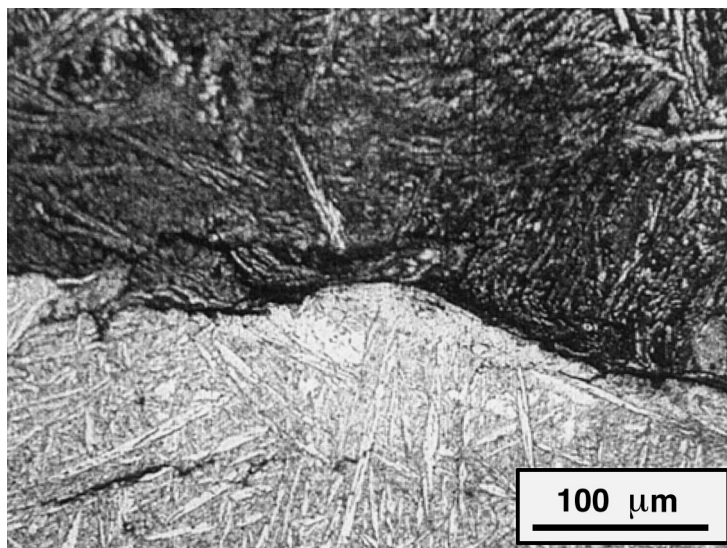


Fig. 3. Optical microstructure of sample after preshock at 24 GPa then spalled at 10 GPa shock pressure. The coexistence of an original and phase-transformed morphology is visible.

stress, but rather increased the temperature of the sample above the thermodynamically estimated temperature for the quenched and aged sample. The adiabatic temperature rise, to the first approximation, can be estimated from the work done on the sample: $w = \int_0^{\epsilon} \bar{\sigma} d\epsilon$, where $\bar{\sigma}$ is flow stress, and ϵ is a strain. Following this $\Delta T = \bar{\sigma}\epsilon/\rho c_p$, where ρ is the material's density, and c_p is its heat capacity. (The temperature estimate using this formula, for the material whose flow stress increases from the quenched, aged, and undeformed condition to the 1700 MPa at about 13% strain (an average of 1300 MPa), gives 515°C, certainly a number comparable to the one calculated using the formulas in Appendix A (555°C)). Thus for a given strain the temperature increases as $\bar{\sigma}$ increases. Therefore, the temperature of the material increased in a spall test with an increase in the flow stress from about $\bar{\sigma} = 1700$ MPa for an quenched aged material to about $\bar{\sigma} = 2700$ MPa due to the preshock, thus to about 885°C (2700 MPa/1700 MPa 555°C = $\sim 885^\circ\text{C}$). This temperature is certainly enough to transform material to γ phase. Such a transformation is necessary for the material to form a eutectoid microstructure upon cooling.

The moderate cooling rate of the shock recovered sample is caused by the large mass of the momentum trapping rings surrounding the sample and recovery system, both designed for the purpose of minimizing residual strains in the sample. After being shock loaded, the samples were recovered from compartments filled with felt soaked in water [3]. These served to decelerate and cool the sample to preserve the microstructure resulting from the shock. Depending on the sample and the momentum trapping rings' sizes the cooling rates

may be nonuniform across the sample. Fig. 3 shows a microscopic view of the coexistence of both the α' martensite laths and the eutectoid $\alpha + \text{U}_2\text{Ti}$ phases obtained from the preshocked and spalled sample. In fact, to obtain the martensitic diffusionless transformation, U–0.75 wt% Ti must be cooled very rapidly and the samples must be rather small (a cooling rate of $\sim 28^\circ\text{C/s}$ is required to obtain 50% martensite – this cooling rate and microstructure would be obtained at the center of 0.5 cm thick sample quenched in water [13]). Our cooling rate was unfortunately not monitored. Fig. 3 microstructure shows cracks running along the phase boundaries. This is an important observation, since it indicates that the thermal expansion coefficients may be different for both phases and the inhomogeneities resulting from the coexistence of two different phases in uranium will have a detrimental effect on the mechanical behavior of this material – for instance causing cracking. How such a coexistence of two phase could occur in this sample?

The are shown in the micrograph was located away from the main spall plane. Therefore the crack separating the $\alpha + \text{U}_2\text{Ti}$ (top) and martensitic microstructures could not have formed in conjunction with the spall event. The logical alternative explanation is that the crack represents the boundary between:

- (a) material that was heated enough to transform to γ -phase, then subsequently cooled at subcritical rates, transforming to $\alpha + \text{U}_2\text{Ti}$ (the top half of Fig. 3), and
- (b) material that was not heated enough to transform to γ -phase, i.e., consists of untransformed martensite present in the original sample (the bottom half of Fig. 3).

Cracking is very likely to occur along an interface as the γ -phase cools and transforms considering, that temperature differences are expected between different portions of the sample due to the stress gradients.

The spall strength of all U–0.75 wt% Ti samples are listed in the caption of Fig. 2. The data show a small decrease in spall strength with increasing shock pressure. The spall strength study on alloyed uranium by Buchar [14] shows similar results. As mentioned before, the preshock generates a high density of defects and raises the yield and flow stresses of the sample; these alone would promote brittle fracture (occasionally found in these samples) and in consequence, would substantially lower the material's spall strength.

4. Summary

The microstructure of the spalled sample preceded by a high strain rate preshock showed eutectoid morphology of $\alpha + U_2Ti$ phase, unlike the samples that were subjected to a spall single cycle, which did not changed their original α' martensite laths morphology.

Acknowledgements

The author would like to acknowledge and thank Dan Thoma and David Embury for stimulating discussions, without which this paper would not be published. George (Rusty) T. Gary III, and the anonymous reviewer are thanked for critically reviewing the manuscript.

Appendix A

Table of symbols:

ΔT	adiabatic temperature increase due to the shock [°C]
E	energy at pressure [Nm/kg or J/kg]
C_p	0.03 [cal/g°C] or [126 J/kg°C], uranium heat capacity
p_0	zero pressure = 0N/m ²
p_p	pressure at shock [N/m ²]
ρ_0	18,930 [kg/m ³], density at zero pressure
ρ_p	density at shock pressure [kg/m ³]
u_p	particle velocity [m/s]
ϑ	750 [m/s], projectile velocity
σ	stress [GPa]
c_0	2510 [m/s], sound velocity in the material at zero pressure
s	1.51 [dimensionless], materials constant – an empirical parameter
U_s	shock velocity [m/s]

The adiabatic temperature increase can be defined as

$$\Delta T = \frac{E}{C_p}, \quad (\text{A.1})$$

where, energy is defined in terms of shock pressure and volume or density change due to the pressure at shock. $\rho_0 = 0$ at zero pressure.

$$E = \frac{1}{2}(p_p - p_0) \left(\frac{1}{\rho_0} - \frac{1}{\rho_p} \right). \quad (\text{A.2})$$

We calculate the particle velocity from the conservation of momentum equation prior to and after the impact, and that equals

$$u_p = \frac{\vartheta}{2}. \quad (\text{A.3})$$

Thus the stress generated by the impact is given by

$$\sigma = \rho_0(c_0 + s u_p) u_p, \quad (\text{A.4})$$

where shock velocity is defined as

$$U_s = c_0 + s u_p. \quad (\text{A.5})$$

The elastic wave propagating at a velocity U_s compresses the material from initial density ρ_0 to ρ_p . The material density at shock is expressed by the following equation:

$$\rho_p = \frac{\rho_0 U_s}{U_s - u_p}. \quad (\text{A.6})$$

The following is the calculation that leads to the temperature rise estimation due to the shock at ~24 GPa shock pressure, achieved in the flat flyer plate 'recovery' compressive preshock experiment at flyer velocity of 750 m/s.

$$u_p = \frac{750}{2} = 375 \text{ m/s, from Eq. (A.3),}$$

$$U_s = 2510 + 1.151 \times 375 = 3076 \text{ m/s, from Eq. (A.5),}$$

$$\rho_p = \frac{18930 \times 3076}{3076 - 375} = 2155 \text{ kg/m}^3, \text{ from Eq. (A.6),}$$

$$\sigma = 18930 \times 3076 \times 375 = 21.8 \text{ GPa, from Eq. (A.4),}$$

$$E = \frac{1}{2} \left(\frac{21.8 \times 10^9 \text{ N}}{\text{m}^2} \right) \left(\frac{\text{m}^3}{18939 \text{ kg}} - \frac{\text{m}^3}{21558 \text{ kg}} \right) \text{ from Eq. (A.2) = } 0.07 \times 10^6 \text{ Nm/kg} = 0.07 \times 10^6 \text{ J/kg}$$

$$C_p = 0.03 \text{ cal/g}^\circ\text{C} = 126 \text{ J/kg}^\circ\text{C},$$

$$\Delta T = \frac{0.007 \times 10^6 \text{ J/kg}}{126 \text{ J/kg}^\circ\text{C}} = 555^\circ\text{C, from Eq. (A.1).}$$

References

- [1] A.K. Zurek, J.N. Johnson, C.E. Frantz, J. Phys. (Paris) 49 (1988) 269.
- [2] G.T. Gray III, P.S. Follansbee, C.E. Frantz, Mater. Sci. Eng. A111 (1989) 9.
- [3] G.T. Gray III, in: J.R. Asay, M. Shahinpoor (Eds.), Influence of Shock-Wave Deformation on the Structure/Property Behavior of Materials, Springer, New York, 1993.

- [4] W.J.M. Rankine, *Philos. Trans.* 160 (1870) 270.
- [5] H.J. Hugoniot, *J. L'Ecole Polytechnic* 58 (1989) 3.
- [6] P.S. DeCarli, M.A. Meyers, in: M.A. Meyers, L.E. Murr (Eds.), *Design of Uniaxial Shock Recovery Experiments*, Plenum, New York, 1980, p. 341.
- [7] A.K. Zurek, *J. Nucl. Mater.* 211 (1994) 52.
- [8] K.H. Eckelmeyer, *Uranium and Uranium Alloys*, ASM International, Materials Park, Ohio, 1985.
- [9] R.G. McQueen, S.P. Marsh, J.W. Taylor, J.N. Fritz, in: R. Kinslow (Ed.), *The Equation of State of Solid from Shock Wave Studies*, Academic Press, New York, 1970, p. 294.
- [10] M.A. Meyers, *Dynamic Behavior of Materials*, Wiley, New York, 1994.
- [11] G.E. Dieter, in: P.G. Shewmon, Z.V.F. (Eds.), *Effects of High-Intensity Shock Waves*, American Institute of Mining, Metallurgical, and Petroleum Engineers, New York, 1961, p. 409.
- [12] A.K. Zurek, P.L. Follansbee, *Metall. and Mater. Trans. A* 26A (1995) 1483.
- [13] K.H. Eckelmeyer, *Uranium and Uranium Alloys*, ASM International, Materials Park, Ohio, 1991.
- [14] J. Buchar, S. Rolc, J. Pechacek, J. Krejci, *J. Phys. (Paris) IV* (1991) 197.